CO$_2$ and H$_2$S Degassing at Fangaia Mud Pool, Solfatara, Campi Flegrei (Italy): Origin and Dynamics of the Pool Basin

Dmitri Rouwet [1,*], **Giancarlo Tamburello** [1] , **Tullio Ricci** [2] , **Alessandra Sciarra** [2] , **Francesco Capecchiacci** [3,4] **and Stefano Caliro** [3]

[1]   Istituto Nazionale di Geofisica e Vulcanologia, Sezione di Bologna, 40128 Bologna, Italy; giancarlo.tamburello@ingv.it

[2]   Istituto Nazionale di Geofisica e Vulcanologia, Sezione di Roma 1, 00143 Rome, Italy; tullio.ricci@ingv.it (T.R.); alessandra.sciarra@ingv.it (A.S.)

[3]   Istituto Nazionale di Geofisica e Vulcanologia, Sezione di Napoli, Osservatorio Vesuviano, 80124 Naples, Italy; francesco.capecchiacci@unifi.it (F.C.); stefano.caliro@ingv.it (S.C.)

[4]   Dipartimento di Scienze della Terra, Università degli Studi di Firenze, 50121 Florence, Italy

*   Correspondence: dmitri.rouwet@ingv.it

Abstract: The Fangaia mud pool provides a "window" into the hydrothermal system underlying the degassing Solfatara crater, which is the most active volcanic centre inside the restless Campi Flegrei caldera, Southern Italy. The present study aimed at unravelling the degassing dynamics of CO$_2$ and H$_2$S flushing through the pH 1.2 steam-heated Fangaia mud pool, an ideal field laboratory as a proxy of an active crater lake. Our results from MultiGAS measurements above Fangaia's surface show that H$_2$S scrubbing, demonstrated by high CO$_2$/H$_2$S ratios, was most efficient in the portions of the basin affected by diffusive degassing. Convective bubbling degassing instead was the most effective mechanism to release gas in quantitative terms, with lower CO$_2$/H$_2$S ratios, similar to the Solfatara crater fumaroles, the high-T end member of the hydrothermal system. Unsurprisingly, total estimated CO$_2$ and H$_2$S fluxes from the small Fangaia pool (~184 m^2 in June 2017) were at least two orders of magnitude lower (CO$_2$ flux < 64 t/d, H$_2$S flux < 0.5 t/d) than the total CO$_2$ flux of the Campi Flegrei caldera (up to 3000 t/d for CO$_2$), too low to affect the gas budget for the caldera, and hence volcano monitoring routines. Given the role of the rising gas as "sediment stirrer", the physical and chemical processes behind gas migration through a mud pool are arguably the creating processes giving origin to Fangaia. Follow-up studies of this so far unique campaign will help to better understand the fast dynamics of this peculiar degassing feature.
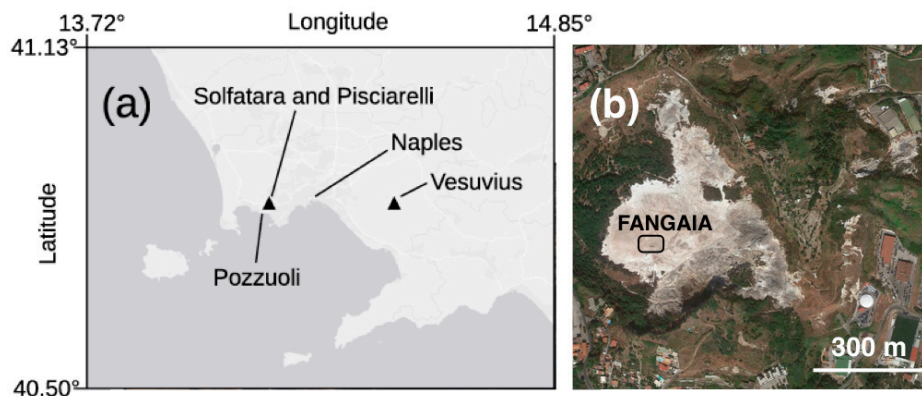
Keywords: Fangaia mud pool; Solfatara; Campi Flegrei; MultiGAS; scrubbing; degassing; geomorphology

1. Introduction

Hot and acidic crater lakes and pools are characterized by evaporation and degassing [1–9]. At pH < 3.8, thermal waters are chemically transparent to CO$_2$, enabling research to trace this deep magmatic marker inside a degassing crater despite the intervening hydrothermal system. In contrast to CO$_2$, H$_2$S and SO$_2$ will be partly scrubbed by the hydrothermal system in the "steam-heated" water phase as a solute S-species (HSO$_4$$^-$-SO$_4$$^{2-}$ thiosulphates, polythionates) or deposited as a solid (elemental S, anhydrite, gypsum, alunites) [10–14].

The Solfatara-Pisciarelli magmatic-hydrothermal system, the most active spot inside the Campi Flegrei caldera (Figure 1a), is renowned for massive CO$_2$ degassing through fumaroles and diffuse soil degassing (up to 858 t/d and 3000 t/d of CO$_2$ [15–19]). Despite being in a non-eruptive state,

recent increases in degassing activity, especially in the dynamic Pisciarelli fumarolic system, have raised concerns that switched the status of Campi Flegrei into the gear of "hydrothermal unrest" [20–22]. The typical magmatic gas species, SO_2, is virtually undetected in any fumarolic gas manifestation, and is presumably efficiently absorbed in deeper aquifers, or reduced in the more superficial hydrothermal system [23,24]. Hence, H_2S is the only S-species emitted at the surface.

Figure 1. Location map of the (**a**) Solfatara and Pisciarelli magmatic-hydrothermal systems, inside the Campi Flegrei caldera, Gulf of Pozzuoli, Naples, and (**b**) Fangaia mud pool inside the Solfatara crater.

The Solfatara crater hosts a muddy lake, Fangaia (Figure 1b), characterized by vigorous bubbling and evaporation, which serves as a "window" into the underlying hydrothermal system. Geophysical surveys revealed that Fangaia is, unsurprisingly, the top of the hydrothermal aquifer underlying the Solfatara crater [25]. The Fangaia mud pool is the surface expression of two different sources of water. The first one consists of liquid, produced by steam condensation in the fumarolic areas (mainly Bocca Grande and Bocca Nuova fumarolic system and Solfatara crypto dome, but also beneath the Fangaia itself), and driven towards the Fangaia topographical depression. The second source is meteoric water [26] flowing inside Solfatara crater that carries solutes from altered deposits and transports them towards the Fangaia basin. The combination of endogenous activity and the presence of altered deposits with peculiar features permit to distinguish the Fangaia subsoil from the surrounding ones within Solfatara crater [27]. From a geochemical point of view, Fangaia is a SO_4-rich (~2000 mg/L) and Cl-poor (<30 mg/L), pH~1.5 steam-heated pool with a temperature between 30 and 47 °C [28].

In this study we aim at revealing the CO_2 and H_2S degassing dynamics at Fangaia, based on MultiGAS measurements conducted right above the surface of the mud pool and executed on 6 June 2017. Although from a quantitative perspective, our determination of the CO_2 output from Fangaia will not massively contribute to the total CO_2 output of Campi Flegrei (i.e., through Solfatara and Pisciarelli fumaroles and diffuse soil degassing [19,20,22]), instead based on variations in CO_2/H_2S ratios above the Fangaia surface, we will provide insights into the kinetics of gases flushing through a hydrothermal system.

## 2. Data Sources: Field, Laboratory and Desk Procedures

We adapted a portable sensor-based gas analyzer (a.k.a. MultiGAS, see [22] for more details on the instrument) by connecting a syringe to a silicon tube sustained by a fishing rod held 2–20 cm above the surface of the Fangaia mud pool (Figure 2). Gas and steam are pumped through the tube into the MultiGAS at a rate of 1.5 L/min. The syringe was held at the same spot for about 20 s to permit the gas to reach the gas analyzer. The measurement procedure (approx. 50 min, Figure 3a) is filmed in time-lapse mode with a GoPRO camera (GoPro Inc., San Mateo, CA, USA, https://gopro.com/), creating a view of the entire area by using a fish-eye lens (Figure 2).

Figure 2. Image showing the field procedure to measure CO_2 and H_2S concentrations above the surface of Fangaia using a fishing rod, long tubing, and a MultiGAS device (MG, left inset). The distances between fluorescent cones are measured in the field (right inset) and the entire field of view is obtained by using fish-eye lens on a GoPRO camera elevated on a tripod.
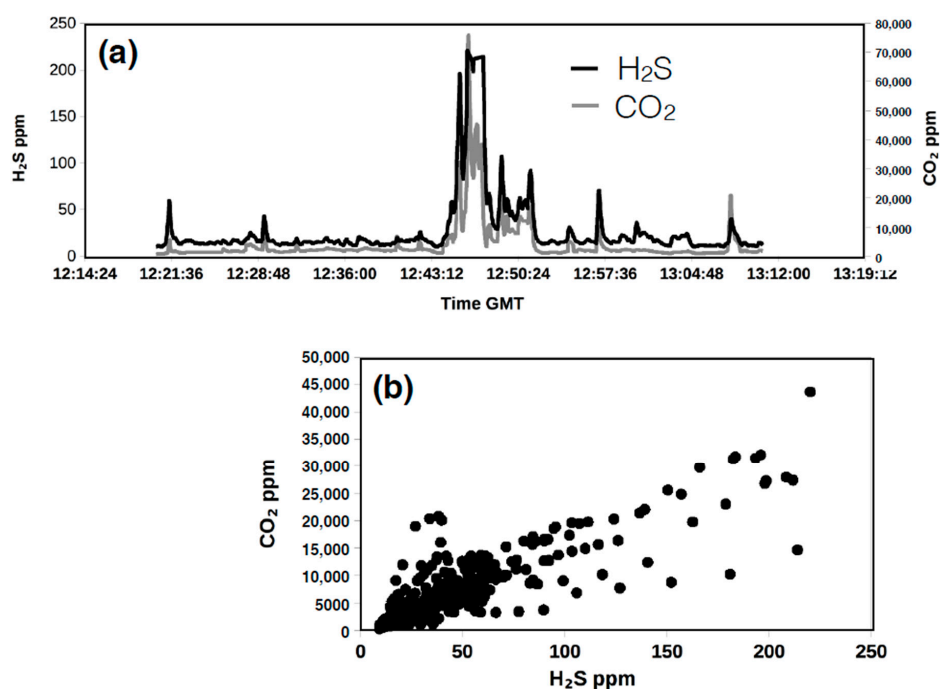
Figure 3. (**a**) temporal variations of CO_2 and H_2S concentrations for 1512 point measurements 2–20 cm above the Fangaia mud pool (green and grey dots in Figure 4), (**b**) CO_2 versus H_2S concentrations using RatioCalc software (https://sites.google.com/site/giancarlotamburello/home) [29].
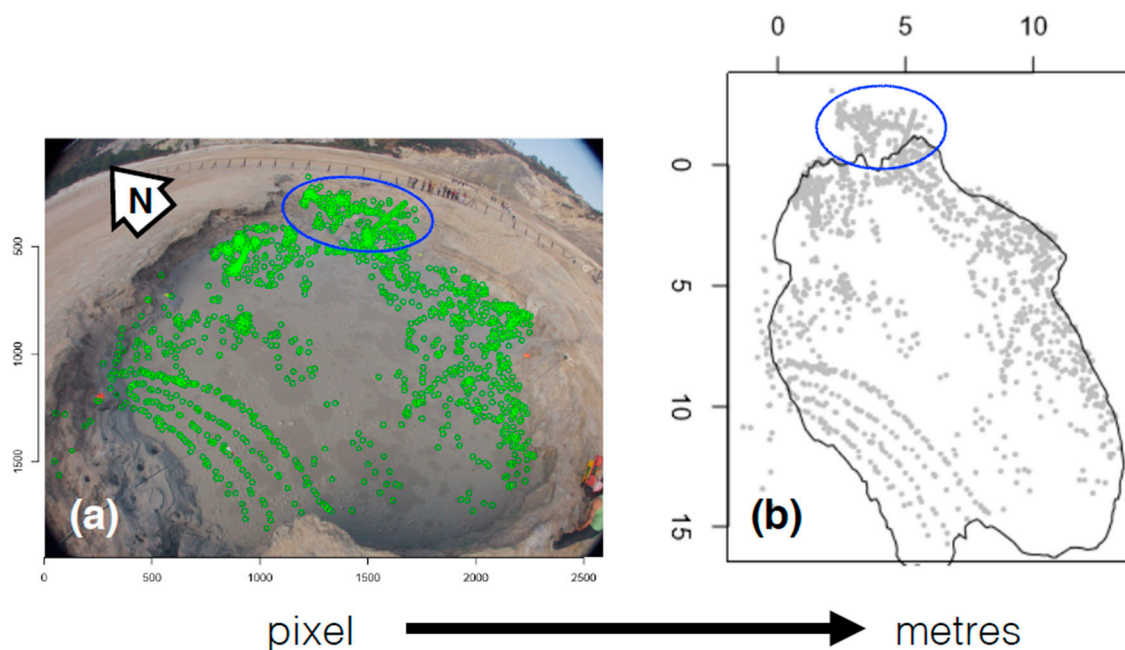
Figure 4. Graphical procedure (MTrackJ and ImageJ software) to mathematically transform pixels (**a**) in the picture into meters (**b**), based on the distances between the fluorescent cones measured in the field. The green (**a**) and grey (**b**) dots are the MultiGAS measurement points. The blue-circle marks the area included in diffuse CO_2 flux measurements, the subaerial degassing area in June 2017 (see Figure 7).

The exact location of the syringe in the image (pixel coordinates) is consequently deduced using the open-source graphical software ImageJ v. 1.8.0_172 (https://imagej.nih.gov/ij/download.html) and MTRackJ v.1.5.1 (https://imagescience.org/meijering/software/mtrackj/) (Figure 4), and converted into metric coordinates with a reference frame established in the field by the clearly visible cones (Figure 2, see [22] for further details). Images are extracted from the GoPRO time-lapse recording with a frequency of 5 s, and are afterwards synchronized to the frequency of data acquisition of the MultiGAS (2 Hz), obtaining a total of 1512 measurements (Figure 3). CO_2 concentrations, corrected for atmospheric background, varied from 320 to 75,800 ppmV, while H_2S concentrations varied from 9.2 ppmV to a saturation value of 224 ppmV (with 36 or 2.3% of the measurement points > 224 ppmV) (Figure 3). The CO_2/H_2S ratios were calculated using the open-source RatioCalc software [29] (Figure 3b). All data were processed to compute the concentration maps in Figure 5 using Kriging as the interpolation method.

The maximum concentrations for both CO_2 and H_2S, measured at <20 cm above the Fangaia surface, are below lethal threshold concentrations (8% and 250 ppmV for CO_2 and H_2S, respectively; except for maximum 2.3% of the H_2S concentrations >224 ppmV, [30]). Moreover, gas concentrations decrease rapidly with height above the surface and do not present any health risk at breathing height for humans.

During our survey in June 2017, the surface area of Fangaia was ~184 m^2. The bathymetry of Fangaia was obtained using 61 direct measurements of the lake depth (Figure 6), and elaborated graphically as above (Figure 4). An operational error of ±5 cm is estimated. The estimated volume of Fangaia was ~75 ± 9 m^3.
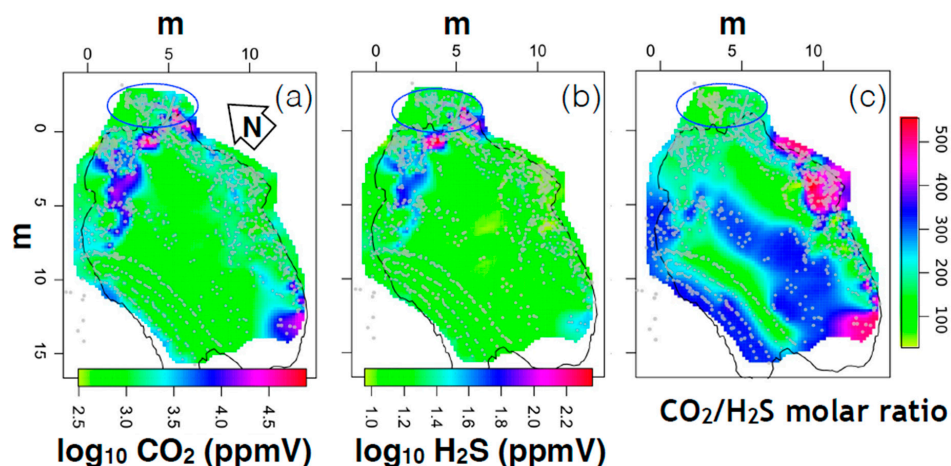
Figure 5. Integrated maps showing the CO_2 (**a**) and H_2S (**b**) concentrations in the air above the Fangaia mud pool. Blue-purple-red colors coincide with stronger degassing areas. The map of CO_2/H_2S ratios (**c**) shows how the stronger degassing areas have the lowest CO_2/H_2S ratios. Highest CO_2/H_2S ratios are detected near the steep-walled shore of Fangaia's basin. The blue-circle marks the area included in diffuse CO_2 flux measurements, the subaerial degassing area in June 2017, "m" indicates meters, for scale.
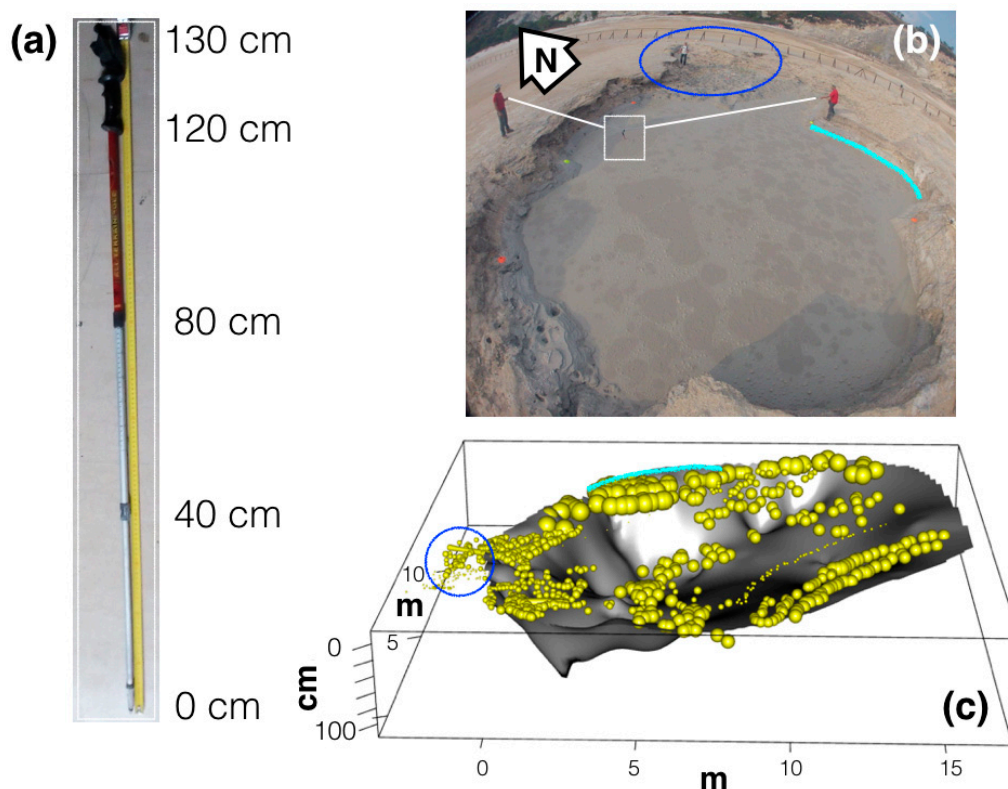
Figure 6. Bathymetry measurements (#61) lowering a scaled walking stick (**a**) attached to ropes from opposite sides of the Fangaia (**b**). (**c**) The resulting bathymetric model as a 3D sketch. The turquoise line in (**b**,**c**) indicate the same shore. The blue ellipse (in (**b**)) and circle (in (**c**)) indicate the dry degassing area.

The CO_2 flux at the degassing (water-free) shores of Fangaia is directly measured using an accumulation chamber [31] equipped with an infrared detector LICOR-LI-820 (LI-COR Biosciences, Lincoln, NE, USA) (Figure 7). These areas are included in the MultiGAS measurements to obtain CO_2 and H_2S concentrations and ratios over areas unaffected by scrubbing.

Figure 7. Direct CO_2 flux measurements (accumulation chamber method by [31]) across the dry section of the Fangaia basin. Note the funnel-shaped vent structures.

The percentage of suspended solids (i.e., "muddiness") in the Fangaia water is obtained after centrifugation (5000 cycles/min), filtering, drying and weighing of the solid phase. Despite the muddy appearance, the small Fangaia contained only 2.85 wt% of solids, defining it as a proxy of a "miniature steam-heated lake".

A water sample was analyzed for its major element composition using ion chromatography (IC; manufacturer at INGV-OV, Napoli, Italy), after centrifugation and filtering in the lab. The pH was measured in the lab by a portable pH meter while the temperature was measured in situ. The steam-heated character (Cl-poor, SO_4-rich) is confirmed by the chemical composition: Na^+ 17 mg/L, K^+ 20 mg/L, Ca^{2+} 48 mg/L, Mg^{2+} 3.9 mg/L, F^- 0.46 mg/L, Cl^- 12 mg/L, SO_4^{2-} 1720 mg/L, NO_3^- 3 mg/L, with a pH of 1.2 and a T of 32 °C, similar to that reported by [28].

3. Discussion

3.1. CO_2 and H_2S Concentrations and CO_2/H_2S Ratios

Figure 5a,b shows integrated concentration maps of CO_2 and H_2S above Fangaia. The highest absolute concentrations for both species were detected above the bubbling areas near the eastern shore of Fangaia, suggesting that most efficient degassing for both species occurs via bubbling. Our expectation of higher CO_2 and H_2S concentrations above the dark colored areas around the center degassing vents was not confirmed by the MultiGAS measurements (Figure 5a,b). Instead, the CO_2/H_2S map reveals low ratios (100–200) above bubbling degassing areas and generally high ratios above diffusively degassing areas (>300; Figures 5c and 8). The CO_2/H_2S ratios above bubbling degassing vents correspond to the ratios observed in the Bocca Nuova and Bocca Grande fumaroles (155 ± 52, for 33 analyses [23]), the high temperature end member (142–163 °C) representative of the Solfatara hydrothermal system, discharging 200 m east of Fangaia. The gas released at the bubbling degassing vents can hence be interpreted as a proxy of the Solfatara fumarole emissions. Remembering that pH 1.2 water is transparent to CO_2, the practically identical CO_2/H_2S ratios of the high-T fumaroles and the bubbling degassing vents imply that H_2S scrubbing in Fangaia is near-nil through bubble gas rise. The trend in varying CO_2/H_2S ratios agrees with a hypothesis of efficient H_2S scrubbing along the water column during slower diffuse, and less efficient scrubbing associated with the relatively rapid rise of bubbling gas. The highest CO_2/H_2S ratios (>400) are detected near the southwestern steep-walled shore of Fangaia (Figures 5c and 8).
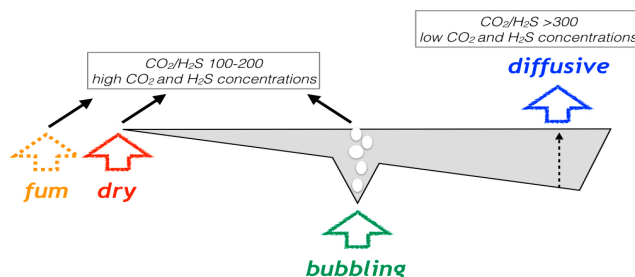
Figure 8. Conceptual model of CO_2/H_2S ratios for the Fangaia basin on 6 June 2017 and the role of bubbling versus diffuse degassing. "Fum" indicates the Bocca Nuova and Bocca Grande fumarole degassing, 200 m off Fangaia; "dry" indicates the degassing area in the dry sector of Fangaia basin, however with lower absolute gas concentrations with respect to the strongest bubbling areas.

A recent study [9] argued that the oxidation state and chemical composition of the gas-receiving lake (El Chichón crater lake in their case) is decisive in the degree of H_2S scrubbing. The very small size of Fangaia, the well-located degassing vents, and the shallow nature of the basin enable a clear differentiation in the response to H_2S scrubbing with respect to the inert CO_2 along the lake surface. In other words, Fangaia is not large and deep enough to homogenize the composition of the gas flushing through the water, as generally is the case at large and deep crater lakes (e.g., Aso, Poás, Kawah Ijen [3,6–8]). Considering Fangaia as a "window" into the Solfatara hydrothermal aquifer, variations in CO_2 fluxes and CO_2/H_2S ratios of soil gases can be affected by the spatial and temporal variations in water saturation levels of the aquifers beneath Solfatara's crater, as well as by the structural control.

3.2. CO_2 and H_2S Fluxes

Three-point flux measurements of diffuse CO_2 soil degassing around Fangaia varied from 8400 g m^{-2} d^{-1} (above the southwestern shores, outside the basin of Fangaia) to 35,600–79,000 g m^{-2} d^{-1} (inside the dried-out basin, near the bubbling degassing vents, shown by the blue ellipses in Figures 4–6). If we tentatively scale these values to the Fangaia area (~184 m^2), we estimate total CO_2 emissions ranging from 6.6 to 14.6 t/d, and an H_2S flux ranging from 0.05 to 0.12 t/d, obtained by dividing the CO_2 flux by the CO_2/H_2S weight ratio of ~100. The latter ratio was measured near the dry sector of the basin (Figure 5c), where the diffuse gas flux measurements were performed.

We also calculated the gas fluxes by integrating the interpolated gas concentrations from Figure 5a and b (the integrated column amount, ICA [32]) and multiplying those values by a plume transport speed. The resulting ICA was 0.75 kg/m for CO_2, and 0.0074 kg/m for H_2S. The plume transport speed was estimated considering that the buoyant rise of a hot volcanic gas ranges from 1 to 3 m/s [32,33], and assuming a rising speed of <1 m/s for the colder gas of the Fangaia. This estimate results in an upper limit for CO_2 and H_2S fluxes of <64 t/d and <0.5 t/d, respectively. The discrepancy between the gas fluxes derived from these two independent methods (i.e., accumulation chamber versus MultiGAS/ICA), suggests that (1) the diffusive gas flux per unit area inside the Fangaia basin might be much higher than the flux detected in the dried-out basin, and/or (2) the buoyant speed of the gas emitted by the Fangaia is much lower than our hypothesized upper limit of 1 m/s. However, our estimates provide an order of magnitude estimate of the gas flux from the Fangaia mud pool, that is comparable to the fluxes of the smaller fumaroles of Solfatara and Pisciarelli [15]. This finding suggests that the degassing of Fangaia does not significantly affect the total CO_2 and H_2S budget, routinely measured during the geochemical monitoring of Campi Flegrei.

3.3. Origin and Dynamics of the Fangaia Basin

Heterogeneous degassing and steam condensation processes ongoing inside the mixed meteoric-hydrothermal aquifer, at the intersection with the Solfatara crater surface, affected by

fracture-controlled diffuse degassing [19], are probably causes of Fangaia's existence. The Fangaia basin was not formed after a (phreatic) eruption, and is hence, by definition, not a crater lake. The many funnel-shaped degassing vents rework sediments and bring them into suspension, creating a mud pool, and leads to an extremely dynamic sedimentary regime. The small basin is highly sensitive to direct rain fall contribution, causing drastic short-term variations in area and volume. E-W and NNE-SSW lineaments cross-cut the area [19]. These lineations in the location of bubbling sites at Fangaia (Figure 5), show it to be part of the Solfatara Diffuse Degassing Structure (DDS [19]), and evidence the structural control on degassing.

Despite the absence of massive CO_2 and H_2S degassing, and the low probability for phreatic eruptions, fast changes in the morphology of the mud pool and its surroundings, and fracture degassing in the area, can lead to the opening of new fractures and fissures. Unfortunately, such rapid fracturing recently occurred after an anomalous rainfall event flooded Fangaia. Three days after, on 12 September 2017, three people died of asphyxiation after falling in a newly formed, poorly ventilated crevasse outside the restricted area of Fangaia. Our June 2017 "snapshot survey", three months prior to the accident, can only reveal the dynamic character of the Fangaia area, but, being first in its kind, could not possibly provide precursory signals in the degassing and morphological-sedimentary regime prior to the accident.

4. Conclusive Remarks

We describe a creative field-based method to measure CO_2 and H_2S concentrations using a MultiGAS immediately above the mud pool Fangaia, in the emblematic Solfatara crater, the most active spot of the restless Campi Flegrei caldera. The small size of the pool (only 184 m^2 in June 2017) and easy access provided (1) an excellent test site for in-field measurements, and (2) insightful results on degassing dynamics of hydrothermal gases flushing through shallow acidic water bodies, a "miniature proxy" to active crater lakes. Diffuse degassing leads to more efficient scrubbing of H_2S and hence higher CO_2/H_2S ratios, whereas bubbling degassing is an inefficient scrubbing mechanism, as indicated by low CO_2/H_2S ratios, to the degree that gasses emitted at the vents are chemically similar to the purest hydrothermal end member released in the Solfatara crater through the Bocca Nuova and Bocca Grande fumaroles. Variations in gas species ratios are diagnostic of changes in volcanic activity. Tracking such variations above the Fangaia bubbling vents can hence become a future monitoring focus.

Contrary to large active crater lakes that seem to show a chemically more homogeneous diffuse plume degassing without bubbling at the surface, the extremely shallow Fangaia highlights heterogeneous degassing through both vigorous gas bubbling and diffusion. Basin depth has arguably a quantitative (gas concentrations and fluxes) and qualitative effect (ratios between gas species) on degassing.

Despite being imposed on top of the hydrothermal system of the Solfatara crater, Fangaia is not a crater lake. The basin itself is formed by intense degassing and steam condensation processes through innumerable funnel-shaped vents, which, in combination with the high sensitivity to rainfall, leads to continuous remobilization of sediments. Rapid changes in morphology of the already weak area can lead to fracturing and destabilization of the basin. A follow-up of this pioneering study is recommended to track possible changes in Fangaia's dynamics, with a focus on (1) geomorphological and hydrological changes with time, on a short- (days) and long-term (months–years) basis, using a water mass balance approach, (2) the relationship between water and gas chemistry, to increase insights into gas scrubbing, (3) possible formation of secondary minerals due to changes in gas-water interactions, and (4) quantifying gas flux and tracking the possible migration of degassing vents, given their physical role of "sediment stirrer", all with the scope to better understand the evolution of the system.

Author Contributions: D.R. field measurements, data analysis, main manuscript drafting; G.T. instrument development, field measurements, data analysis, manuscript drafting; T.R. field measurements, manuscript drafting; A.S. field measurements, data analysis; F.C. water sample analysis, manuscript drafting; S.C. manuscript drafting, responsible funding. All authors have read and agreed to the published version of the manuscript.

Conflicts of Interest: The authors declare no conflict of interest.

References

1. Rouwet, D.; Tassi, F.; Mora-Amador, R.; Sandri, L.; Chiarini, V. Past, present and future of volcanic lake monitoring. *J. Volcanol. Geotherm. Res.* **2014**, *272*, 78–97. [CrossRef]

2. Rouwet, D.; Ohba, T. Cl partitioning and isotopic fractionation during crater lake fluid cycling. In *Volcanic Lakes*; Rouwet, D., Christenson, B., Tassi, F., Vandemeulebrouck, J., Eds.; Springer: Heidelberg, Germany, 2015; pp. 179–200. [CrossRef]

3. Shinohara, H.; Yoshikawa, S.; Miyabuchi, Y. Degassing activity of a volcanic crater lake: Volcanic plume measurements at the Yudamari crater lake, Aso volcano, Japan. In *Volcanic Lakes*; Advances of Volcanology IAVCEI Series; Springer: Heidelberg, Germany, 2015. [CrossRef]

4. Tamburello, G.; Agusto, M.; Caselli, A.; Tassi, F.; Vaselli, O.; Calabrese, S.; Rouwet, D.; Capaccioni, B.; Di Napoli, R.; Cardellini, C.; et al. Intense magmatic degassing through the lake of Copahue volcano, 2013–2014. *J. Geophys. Res.* **2015**. [CrossRef]

5. Capaccioni, B.; Rouwet, D.; Tassi, F. HCl degassing from extremely acidic crater lakes: Empirical results from experimental determinations and implications for geochemical monitoring. In *Geochemistry and Geophysics of Volcanic Lakes*; Caudron, C., Capaccioni, B., Ohba, T., Eds.; Geological Society of London Special Publications: London, UK, 2017. [CrossRef]

6. de Moor, J.M.; Aiuppa, A.; Pacheco, J.; Avard, G.; Kern, C.; Liuzzo, M.; Martínez, M.; Giudice, G.; Fischer, T.P. Short-period volcanic gas precursors to phreatic eruptions: Insights from Poás volcano, Costa Rica. *Earth Planet. Sci. Lett.* **2016**, *442*, 218–227. [CrossRef]

7. de Moor, J.M.; Stix, J.; Avard, G.; Muller, C.; Corrales, E.; Diaz, J.A.; Alan, A.; Brenes, J.; Pacheco, J.; Aiuppa, A.; et al. Insights on hydrothermal-magmatic interactions and eruptive processes at Poás volcano (Costa Rica) from high-frequency gas monitoring and drone measurements. *Geophys. Res. Lett.* **2019**, *46*, 1293–1302. [CrossRef]

8. Gunawan, H.; Caudron, C.; Pallister, J.; Primulyana, S.; Christenson, B.; McCausland, W.; van Hinsberg, V.; Lewicki, J.; Rouwet, R.; Kelly, P.; et al. New insights into Kawah Ijen's volcanic system from the wet volcano workshop experiment. In *Geochemistry and Geophysics of Volcanic Lakes*; Caudron, C., Capaccioni, B., Ohba, T., Eds.; Geological Society of London Special Publications: London, UK, 2017. [CrossRef]

9. Hasselle, N.; Rouwet, D.; Aiuppa, A.; Jácome-Paz, M.P.; Pfeffer, M.; Taran, Y.; Campion, R.; Bitetto, M.; Giudice, G.; Bergsson, B. Sulfur degassing from steam-heated crater lakes: El Chichón (Chiapas, Mexico) and Víti (Iceland). *Geophys. Res. Lett.* **2018**, *45*, 7504–7513. [CrossRef]

10. Takano, B. Correlation of volcanic activity with sulfur oxyanion speciation in crater lake. *Science* **1987**, *235*, 1542–1712. [CrossRef]

11. Symonds, R.B.; Gerlach, T.M.; Reed, M.H. Magmatic gas scrubbing: Implications for volcano monitoring. *J. Volcanol. Geotherm. Res.* **2001**, *108*, 303–341. [CrossRef]

12. Kusakabe, M.; Komoda, Y.; Takano, B.; Abiko, T. Sulfur isotopic effects in the disproportionation reaction of sulfur dioxide in hydrothermal fluids: Implications for the $\delta 34S$ variations of dissolved bisulfate and elemental sulfur from active crater lakes. *J. Volcanol. Geotherm. Res.* **2000**, *97*, 287–307. [CrossRef]

13. Delmelle, P.; Bernard, A. The remarkable chemistry of sulfur in hyper-acid crater lakes: A scientific tribute to Bokuichiro Takano and Minoru Kusakabe. In *Volcanic Lakes*; Advances in Volcanology IAVCEI Series; Rouwet, D., Christenson, B., Tassi, F., Vandemeulebrouck, J., Eds.; Springer: Heidelberg, Germany, 2015. [CrossRef]

14. Inguaggiato, C.; Pappaterra, S.; Peiffer, L.; Apollaro, C.; Brusca, L.; De Rosa, R.; Rouwet, D.; Caudron, C. Suparjan Mobility of REE from a hyperacid brine to secondary minerals precipitated in a volcanic hydrothermal system: Kawah Ijen crater lake (Java, Indonesia). *Sci. Total Environ.* **2020**, *740*. [CrossRef]

15. Aiuppa, A.; Tamburello, G.; Di Napoli, R.; Cardellini, C.; Chiding, G.; Giudice, G.; Grassa, F.; Pedone, M. First observations of the fumarolic gas output from a restless caldera: Implications for the current period of unrest (2005–2013) at Campi Flegrei. *Geochem. Geophys. Geosyst.* **2013**, *14*, 4153–4169. [CrossRef]

16. Pedone, M.; Aiuppa, A.; Giudice, G.; Grassa, F.; Cardellini, C.; Chiodini, G.; Valenza, M. Volcanic CO_2 flux measurement at Campi Flegrei by tunable diode laser absorption spectroscopy. *Bull. Volcanol.* **2014**, *76*. [CrossRef]

17. Aiuppa, A.; Fiorani, L.; Santoro, S.; Parracino, S.; Nuvoli, M.; Chiodini, G.; Minopoli, C.; Tamburello, G. New ground-based lidar enables volcanic CO_2 flux measurements. *Sci. Rep.* **2015**, *5*. [CrossRef] [PubMed]

18. Queißer, M.; Granieri, D.; Burton, M. A new frontier in CO_2 flux measurements using a highly portable DIAL laser system. *Sci. Rep.* **2016**, *6*, 33834. [CrossRef]

19. Cardellini, C.; Chiodini, G.; Frondini, F.; Avino, R.; Bagnato, E.; Caliro, S.; Lelli, M.; Rosiello, A. Monitoring diffuse volcanic degassing during volcanic unrests: The case of Campi Flegrei (Italy). *Sci. Rep.* **2017**, *7*, 6757. [CrossRef]

20. Chiodini, G.; Vandemeulebrouck, J.; Caliro, S.; D'Auria, L.; De Martino, P.; Mangiacapra, A.; Petrillo, Z. Evidence of thermal-driven processes triggering the 2005–2014 unrest at Campi Flegrei caldera. *Earth Planet. Sci. Lett.* **2015**, *414*, 58–67. [CrossRef]

21. Chiodini, G.; Giudicepietro, F.; Vandemeulebrouck, J.; Aiuppa, A.; Caliro, S.; De Cesare, W.; Tamburello, G.; Avino, R.; Orazi, M.; D'Auria, L. Fumarolic tremor and geochemical signals during a volcanic unrest. *Geology* **2017**, *45*, 1131–1134. [CrossRef]

22. Tamburello, G.; Caliro, S.; Chiodini, G.; De Martino, P.; Avino, R.; Minopoli, C.; Carandente, A.; Rouwet, D.; Aiuppa, A.; Costa, A.; et al. Escalating CO_2 degassing at the Pisciarelli fumarolic system, and implications for the ongoing Campi Flegrei unrest. *J. Volcanol. Geotherm. Res.* **2019**, *384*, 151–157. [CrossRef]

23. Caliro, S.; Chiodini, G.; Moretti, R.; Avino, R.; Granieri, D.; Russo, M.; Fiebig, J. The origin of the fumaroles of La Solfatara (Campi Flegrei, South Italy). *Geochim. Cosmochim. Acta* **2007**, *71*. [CrossRef]

24. Giggenbach, W.F. Redox processes governing the chemistry of fumarolic discharges from White Island, New Zealand. *Appl. Geochem.* **1987**, *2*, 143–161. [CrossRef]

25. Bruno, P.P.G.; Ricciardi, G.P.; Petrillo, Z.; Di Fiore, V.; Troiano, A.; Chiodini, G. Geophysical and hydrogeological experiments from a shallow hydrothermal system at Solfatara Volcano, Campi Flegrei, Italy: Response to caldera unrest. *J. Geophys. Res.* **2007**, *112*, B06201. [CrossRef]

26. Gresse, M.; Vandemeulebrouck, J.; Byrdina, S.; Chiodini, G.; Revil, A.; Johnson, T.C.; Ricci, T.; Vilardo, G.; Mangiacapra, A.; Lebourg, T.; et al. Three-dimensional electrical resistivity tomography of the Solfatara Crater (Italy): Implications for the multiphase flow structure of the shallow hydrothermal system. *J. Geophys. Res. Solid Earth* **2017**, *122*, 8749–8768. [CrossRef]

27. Montanaro, C.; Mayer, K.; Isaia, R.; Gresse, M.; Scheu, B.; Yilmaz, T.I.; Vandemeulebrouck, J.; Ricci, T.; Dingwell, D.B. Hydrothermal activity and subsoil complexity: Implication for degassing processes at Solfatara crater, Campi Flegrei. *Bull. Volcanol.* **2017**. [CrossRef]

28. Aiuppa, A.; D'Alessandro, W.; Federico, C.; Palumbo, B.; Valenza, M. The aquatic geochemistry of arsenic in volcanic groundwaters from southern Italy. *Appl. Geochem.* **2003**, *18*, 1283–1296. [CrossRef]

29. Tamburello, G. Ratiocalc: Software for processing data from multicomponent volcanic gas analyzers. *Comput. Geosci.* **2015**, *82*, 63–67. [CrossRef]

30. Available online: https://www.ivhhn.org/information/information-different-volcanic-gases (accessed on 23 November 2020).

31. Chiodini, G.; Cioni, R.; Guidi, M.; Raco, B.; Marini, L. Soil CO_2 flux measurements in volcanic and geothermal areas. *Appl. Geochem.* **1998**, *13*, 543–552. [CrossRef]

32. Tamburello, G.; Aiuppa, A.; Kantzas, E.P.; McGonigle, A.J.S.; Ripepe, M. Passive vs. active degassing modes at an open-vent volcano (Stromboli, Italy). *Earth Planet. Sci. Lett.* **2012**, *359–360*, 106–116. [CrossRef]

33. Delle Donne, D.; Tamburello, G.; Aiuppa, A.; Bitetto, M.; Lacanna, G.; D'Aleo, R.; Ripepe, M. Exploring the explosive-effusive transition using permanent ultraviolet cameras. *J. Geophys. Res. Solid Earth* **2017**, *122*, 4377–4394. [CrossRef]